Carbohydrate Polymers 80 (2010) 105–114

Contents lists available at ScienceDirect

Carbohydrate Polymers

journal homepage: www.elsevier.com/locate/carbpol

Hydroxypropyl methylcellulose (HPMC) formulated films: Relevance to adhesion and friction surface properties

Ahmad Fahs, Maurice Brogly *, Sophie Bistac, Marjorie Schmitt

Laboratoire de Chimie Organique Bio-organique et Macromoléculaire COBM, Ecole Nationale Supérieure de Chimie de Mulhouse ENSCMu, 3 rue Alfred Werner, 68093 Mulhouse cedex, France

ARTICLE INFO

Article history:
Received 28 July 2009
Received in revised form 13 October 2009
Accepted 29 October 2009
Available online 5 November 2009

Keywords:
Hydroxypropyl methylcellulose
Stearic acid
Adhesion
Friction
Atomic force microscopy
Nanoscale/macroscale

ABSTRACT

Cellulose derivatives constitute one of the most dedicated polymers used in the production of film coatings (tablets, capsules . . .). The effect of the composition of hydroxypropyl methylcellulose (HPMC)-stearic acid films on the surface physico-chemical properties was investigated. Incorporation of stearic acid into HPMC films induces strong changes on surface structure, hydrophobic/hydrophilic character, adhesion and friction characteristics. The variations observed suggest an accumulation of stearic acid on film surfaces, resulting a decrease of its roughness and surface free energy. The nano-adhesion and nano-friction experiments were evaluated by using AFM/FFM, while the macro-adhesion and macro tribological studies were performed on tack test and pin-on-disk tribometer respectively. In all the cases, it was found that the hydrophobic character of stearic acid leads to decrease adhesion and friction at the two scales. The surface capillary force plays a key role in these properties. In addition, the study indicates the interplay of adhesion in friction property of HPMC films and the role of stearic acid as lubricant.

1. Introduction

Cellulose derivatives are used in a wide variety of applications fields such as food, pharmaceutical, textile, and adhesive industries. They constitute one of the most dedicated polymers used in the production of film coatings (Ott, Spurlin, & Graffin, 1954; Smith, 2005). High-purity grades are marketed for applications in the food, pharmaceutical and cosmetics sectors.

Cellulose derivatives are often used to modify the release of drugs in tablet and capsule formulations (Doelker, 1993; Kamel, Ali, Jahangir, Shah, & El-Gendy, 2008). Hydroxypropyl methylcellulose (HPMC) is the most extensively employed because of its ease of use, availability, water solubility, and non-toxicity. It is primarily used as a controlled release matrix (Ford, 1999). Drug release from these systems is controlled by the hydration of HPMC, which forms a gelatinous layer at the surface of the matrix through which the included drug diffuses (Sakellariou & Rowe, 1995; Tahara, Yamamoto, & Nishihata, 1995). Vegetarian capsules based on HPMC films constitute an interesting product and recently the research to develop these types of capsules become more active. These capsules are commercially available, mainly to the dietary supplement industry as a "green" alternative to gelatin (Ogura, Furuya, & Matsuura, 1998). HPMC is classified according to the content of substituents and its viscosity. The substitution affects the solubility–temperature relationship and its selection is important for some pharmaceutical applications. HPMC is soluble in cold water and some organic solvents and over the entire biological pH range. HPMC forms transparent, tough and flexible films from aqueous solutions (McGinity & Felton, 2008).

Additives are often incorporated to improve specific properties of formulated films. Additives into films includes plasticizers (Aulton, Abdul-Razzak, & Hogan, 1981; Debeaufort & Voilley, 1997; Navarro-Tarazaga, Sothornvit, & Pérez-Gago, 2008; Okhamafe & York, 1983), surfactants (Pérez, Carrera Sánchez, Rodríguez Patino, & Pilosof, 2006; Villalobos, Chanona, Hernandez, Gutiérrez, & Chiralt, 2005; Villalobos, Hernandez-Munoz, & Chiralt, 2006), antimicrobial agents (Sebti, Ham-Pichavant, & Coma, 2002; Torres, Motoki, & Karel, 1985) and pigments (Bechard, Quraishi, & Kwong, 1992). Several studies have focused on the influence of additives on physico-chemical properties of HPMC films. It is known that lipid compounds such as waxes, triglycerides (e.g., tristearin), fatty acids (e.g., stearic and palmitic acid), frequently incorporated into HPMC films, lead to a decrease in the water affinity and moisture transfer due to their high hydrophobic properties caused by their high content of long-chain fatty alcohols and alkanes. Stearic acid represents a model molecule for which manufacturers are particularly interesting (Ayranci & Tunc, 2001; Coma, Sebti, Pardon, Deschamps, & Pichavant, 2001; Hagenmaier & Shaw, 1990). The properties of fatty acids and of lipids derived from them are markedly dependent on their physical state, chain length, and degree of saturation. Unsaturated fatty acids have a significantly lower melting point than saturated fatty acids of the same chain length (18 carbons). For example, the melting point of stearic acid is 69.6 °C,

* Corresponding author. Tel.: +33 (0)3 89 33 69 18; fax: +33 (0)3 89 42 32 82.
E-mail address: maurice.brogly@uha.fr (M. Brogly).

0144-8617/$ - see front matter © 2009 Elsevier Ltd. All rights reserved.
doi:10.1016/j.carbpol.2009.10.071

whereas those of oleic, linoleic, and linolenic acids are 16.3, −5, and −11 °C, respectively. Plasticizers are used for softening films, reducing brittleness, increasing flexibility and modifying thermal properties (Aulton et al., 1981; Debeaufort & Voilley, 1997; Navarro-Tarazaga et al., 2008; Okhamafe & York, 1983).

Surface properties of materials play an important role when the products are used into domains such as pharmaceutical. Nevertheless, very few studies concern surface properties of HPMC formulated films. The present study focuses on the understanding of the effects of hydrophobic additive on the surface characteristics of the formulated films. Surface characteristics will be explored in terms of structuration, surface morphologies, surface phase separation, surface energy, adhesion and sliding properties, on both nano and macro scales. As a fatty acid, we have chosen the stearic acid, a saturated fatty acid that has 18 carbon atoms, used in formulated films at concentrations less than 1% w/w (Gad, 2008).

The aim of the present study is to investigate the surface properties of HPMC films formulated with a fatty acid as additive and understand at a very local scale, how a hydrophobic additive impact the surface properties of new green-based film coatings. Moreover a second objective concerns the correlations between nanoscale and macroscale surface properties. In order to control the hydrophobicity/hydrophilicity of the surface, the effects of additive concentration on wettability, adhesion and friction behaviors are discussed. The HPMC formulated films are analyzed by using contact angle to evaluate films wettability. Atomic force microscopy in tapping mode TM-AFM was used to explore surface morphology. Adhesion and friction measurements at nanoscale were performed by chemical force microscopy (CFM) and friction force microscopy (FFM) respectively. At macroscale, tack test and a pin-on-disk friction test were conducted to access adhesion and tribological properties respectively.

2. Materials and methods

Hydroxypropyl methylcellulose (Methocel E3 Premium LV) was manufactured by Dow Chemical Company and kindly supplied by Colorcon – France. This HPMC satisfies the standards of the United States Pharmacopoiea USP and European Pharmacopoiea. HPMC is white to slightly white granular powder, soluble in cold water and insoluble in hot water. HPMC polymers are available in a number of viscosity grades, defined as the nominal viscosity of a 2% w/w aqueous solution at 20 °C. In the present study, we used the grade which has a nominal viscosity of 3 mPa s. The degree of substitution (DS) is defined as the average number of hydroxyl groups substituted per anhydroglucose unit. The DS of HPMC used for methoxyl and hydroxypropyl substitutions is equal to 1.91 and 0.25, respectively. It can be also defined in terms of weight percent; the amount of OCH_3 group is 28.8% (w/w) and hydroxypropyl group is 9.1% (w/w). The methoxyl group OCH_3 is still the major substituent of the anhydroglucose units of cellulose. The hydroxypropyl substituent group, $-OCH_2CH(OH)CH_3$, contains a secondary hydroxyl and may also be considered to form a propylene glycol ether of cellulose (Fig. 1). The quantification of methoxyl and hydroxypropoxyl contents was already carried out by infrared and ^{13}C NMR spectroscopy. NMR spectroscopy is powerful and allows precise quantification of the degree of substitution relative to each glucopyranose hydroxyl. The DS and the nature of substituents influence properties such as organic solubility and the thermal gelation temperature of aqueous solutions. HPMC polymer has a high glass transition temperature T_g as determined by differential scanning calorimetry DSC after evaporation of water content. T_g depends on the molecular weight of HPMC polymers. The T_g obtained for HPMC polymer which has 10,000 g/mol molecular weight is 138 °C.

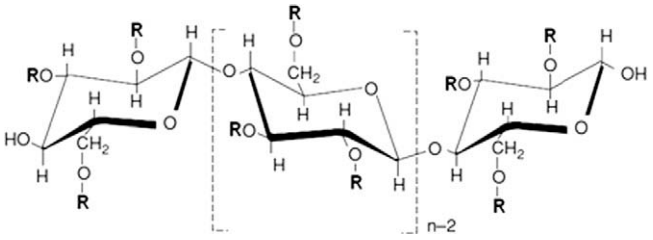

Fig. 1. Chemical structure of hydroxypropyl methylcellulose R=H, $-CH_3$ or $-(OCH_2CHCH_3)_xOH$.

Stearic acid (Sigma Chemical Company, purity 99%) was used for film formation without supplementary purification.

2.1. Film formation

HPMC films were obtained by casting, where the polymer solution is cast onto an anti-adhesive substrate. The solvent is evaporated by natural convection. To prepare pure HPMC films, HPMC solution (6% w/v) was prepared by dispersing HPMC powder under moderate agitation in deionised water at 80–90 °C to prevent lumping, as a vigorous agitation cause severe foaming which may be difficult to remove. HPMC was dissolved by hydration and cooling to 25 ± 2 °C. A clear solution is obtained after cooling. To formulate HPMC–stearic acid films, HPMC solution with stearic acid was prepared by dissolving stearic acid in 10 ml absolute ethanol and adding it to HPMC solution. The amount of stearic acid is given as a percentage of HPMC powder (0.1%, 0.5% and 1% w/w HPMC). The solution was then homogenized for 2 h. To achieve the maximum hydration of HPMC polymer, all solutions were preserved at 5 °C for 24 h.

To obtain 100 μm thick films, solutions were poured in an uniform layer of 1.6 mm thickness onto a glass plate. Films were formed by drying at natural convection for 48 h. The dried films were peeled from the glass plates and samples were conditioned at 25 ± 2 °C and 30 ± 5% RH before experiments.

2.2. Contact angle measurements

Contact angles were measured with the sessile drop technique, by depositing a drop of a liquid onto the film surface. The drop is imaged and the resulting contact angle is determined by drop shape image analysis calculation. The instrument used is a Krüss G2 Goniometer. The contact angle measurements were carried out in open air at a relative humidity of 30 ± 5% RH and at a room temperature of 22 ± 2 °C by using three liquids: water, diiodomethane and α-bromonaphtalene. The volume of droplets is in the range 2–3 μl. Ten droplets were imaging at different regions of the same piece of film. The contact angle is averaged over these 10 values. Measurements of contact angle will allow us to calculate the surface free energy of formulated films.

2.3. Surface free energy

The surface free energy was determined from the experimental contact angles and surface tensions of the probe liquids. Owens and Wendt (1969) extended the ideas of Fowkes (1963) to cases where both dispersion and polar forces operated. The approach of Owens and Wendt was coupled with Young's equation to result in:

$$\gamma_l(1+\cos\theta) = 2\left(\gamma_s^d\gamma_l^d\right)^{1/2} + 2\left(\gamma_s^p\gamma_l^p\right)^{1/2} \quad (1)$$

where θ is the contact angle of the liquid on the film solid surface γ_l^d and γ_l^p, respectively, are the dispersive and polar components of the surface free energy of the liquid, and γ_l is the surface free energy of

Table 1
Dispersive and polar components and surface free energy of different liquids used in contact angle measurement (mJ m^{-2}).

Liquid	Dispersive component	Polar component	Surface free energy
Water	21.8	51	72.8
Diiodomethane	46.6	4.2	50.8
α-bromonaphtalene	44.6	0	44.6

the liquid. Table 1 summarizes the surface free energy and the polar and dispersive components of the different probe liquids.

The dispersive component of the surface energy of the film solid surface (γ_s^d) is calculated from contact angle measured with a purely dispersive liquid. The polar component (γ_s^p) is determined by making contact angle measurements with a polar liquid. Surface free energy is the sum of the polar and dispersive components of the surface energy.

2.4. Atomic force microscopy (AFM)

The AFM has become a usual surface profiler for topographic and normal force measurements on the micro to nanoscale. Interaction forces, attractive or repulsive, as small as few nano-Newtons between the tip and the sample can be measured. In our study, the AFM experiments were carried out using a Nanoscope IIIa controller (Digital Instruments, Santa Barbara, CA) in both tapping and contact mode in order to access surface topography, hydrophilic/hydrophobic character of the surface as well as adhesive and friction properties at the nanoscale (Birdi, 2003).

2.4.1. Topographical measurements

Topography measurements of HPMC films is realized by tapping mode (intermittent contact mode), also referred to as dynamic force microscopy. In this mode, during scanning over the surface, the cantilever/tip assembly is sinusoidally vibrated by a piezo mounted above it, and the oscillating tip slightly taps the surface at the resonant frequency of the cantilever with a constant oscillating amplitude introduced in the vertical direction with a feedback loop keeping the average normal force constant (Bhushan, 2005). During scanning sample, AFM tip encounters the attractive and the repulsive force fields. Topographical measurements are made at fixed scanning angle equal to 0°.

In our measurements, we used silicon probes (Veeco probes), with a spring constant of 5 N m^{-1}, a resonance frequency of 150 kHz and tip radius of 10 nm. All images were collected with a resolution of 512 × 512 pixels and scan rate of 0.8 Hz for 1 μm × 1 μm images. All experiments were performed in air at ambient conditions.

2.4.2. Adhesion at nanoscale

To measure adhesion between two solid surfaces, one of them is suspended on a spring and the adhesion or "pull-of" force needed to separate the two surfaces is deduced knowing the deflection of the spring. In the case of AFM where the first surface is the AFM tip and the second is the substrate, interaction forces between them are calculated through the application of Hooke's law: $F = k{\cdot}\Delta z$, where k is cantilever spring constant (N/m) and Δz is cantilever deflection (nm) (Bhushan, 2005).

The measurement of adhesion force at the nanoscale between tip and HPMC formulated films was performed in contact mode AFM by recording force curve. Silicon nitride Si_3N_4 cantilevers of 115 μm length, 57 kHz resonance frequency with pyramidal sharpened tips were used. The spring constant was 0.3 N m^{-1} and the radius of curvature of the tip was 45 nm. Calibration of the spring constant cantilevers is of major importance to calculate adhesion force and to obtain quantitative and reliable data.

2.4.3. Force–distance curve measurements

Force measurements with AFM, in the contact mode, consist in detecting the deflection of a spring (or cantilever) bearing a silicon nitride tip at its end, when interacting with the sample surface. The deflection of the cantilever is detected by an optical device (four quadrants photodiode) while the tip is vertically moved forward and backward thanks to a piezoelectric ceramic (or actuator). Thus, provided that the spring constant of the cantilever is known, one can obtain a deflection–distance (DD) curve and then a Force–Distance (FD) curve, by using Hooke's law. A schematic representation of a DD curve obtained when probing a hard surface is reported in Fig. 2.

In zone A, the cantilever is far from the surface and stays in a state of equilibrium (no interaction with the surface). The cantilever deflection is zero. During the approach to (or withdrawal from) the surface, the tip interacts with the sample and a jump-in (or jump-off) contact occurs (zones B (for loading) and E (for unloading)). These instabilities take place because the cantilever becomes mechanically unstable. Usually, for underfomable surfaces, because of mechanical instabilities, jump-in contact is not significant to determine attractive Van der Waals forces. When in contact, the cantilever deflection is equal to the piezoelectric ceramic displacement provided no indentation of the substrate occurs (zones C (for loading) and D (for unloading)). An underfomable reference sample (cleaned silicon wafer) is used to scale the DD curve in deflection by fixing to unity the slope value of the contact line. Due to adhesion forces during contact, the jump-off is greater than the jump-in and occurs in position D. Considering the cantilever like a spring, knowing its spring constant, one can obtain the adhesion force between the tip and the sample by using Hooke's law:

$$F = k \cdot \Delta z \tag{2}$$

where, k represents the spring constant of the cantilever and Δz represents the jump-off during retraction of the tip from the surface.

The reported force values are the averages of 30 measurements at different locations on the HPMC films. All measurements were made using the same AFM tip. In order to carry out a quantitative analysis, different experimental points should be taken into consideration such as: cantilever spring constant, tip radius, linearity of the photodiodes, piezo driver hysteresis, cantilever and piezo thermal stabilities and tip contamination (Brogly, Noel, Awada, Castelein, & Schultz, 2006).

2.4.4. Determination of the spring constant of the cantilever

It was performed using two methods: micromachined cantilevers with a known spring constant and thermal noise method. For the first one, we have chosen the method proposed by Torii, Sasaki, Hane and Okuma (1996)) for its simplicity. This non-destructive method refers to the use of rectangular reference cantilevers (calibrated with the resonant frequency method and

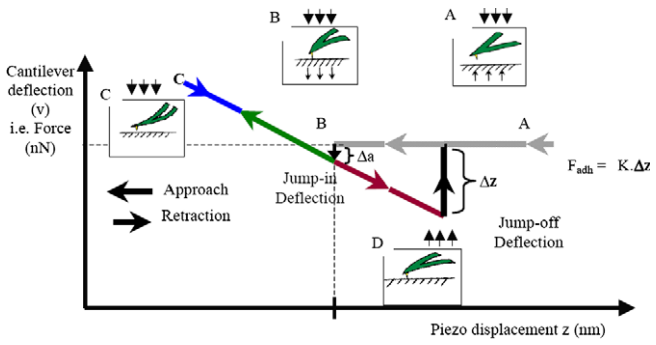

Fig. 2. Representation of deflection–distance (DD) curve.

supplied by Veeco, France). Calibration of the pyramidal shaped tips used for probing nano-adhesion (supplied by Veeco, France) gives an effective spring constant equal to 0.30 ± 0.03 N m^{-1} (the value specified by the supplier is 0.58 N m^{-1}!).

Spring constants of cantilevers were also measured using a software routine based upon the measurement of the thermal oscillations of the cantilever (Hutter & Bechhoefer, 1993) (by using Nanoscope V). Obtained values agree with those previously determined: 0.3 ± 0.03 N m^{-1}.

2.4.5. Nonlinearity of the quadrant of photodiodes

The nonlinearity of the optical detector is the consequence of a non-homogeneous spreading of the laser spot on the detector. This nonlinearity has been studied by reporting the slope of the contact line (zones C or D) of the DD curve (obtained on a hard surface and considering that there is no nonlinearity at the middle of the photo detector) versus the tension (V) measured by the detector. The domain of linearity of the detector lies between ±2 V. If nonlinearity is not taken into account, the error on the quantitative results can be significant, because the slope of the contact line determines the Y-scale.

2.4.6. Scan rate of the cantilever

The piezodriver used to move the cantilever vertically and forward shows hysteresis and nonlinearity in its vertical displacement. This hysteresis can be studied by reporting the slope of the contact zones (zones C and D) versus the amplitude of the contact zone and the scan rate. During the experiments, the actuator is considered as thermally stable. We observed that a discrepancy appears for very low scan rates (60 nm s^{-1}). For higher scan rates (18 μm s^{-1}), the viscosity of the environment could be significant (damping effect). A rate of about 6 μm s^{-1} is a good compromise. In order to stabilize thermally the piezodriver, the machine is turned on 12 h before. Contamination of the tip was checked by measuring adhesion force between the tip and a reference surface after each 30 Force–Distance curves realized on HPMC films.

2.5. Friction at nanoscale

Friction force microscopy FFM is a powerful research tool for the surface characterization of materials and helps to explain friction phenomena at the nanoscale. The sample is scanned back and forth (producing a friction loop) in a direction perpendicular to the long axis of the cantilever. The friction force between the films and the tip produces a twisting of the cantilever.

Nanoscale friction is quantified by TMR (Trace Minus Retrace, in Volts, equal to the difference between lateral forces scanning left-to-right and right-to-left). The lateral spring constant depends critically on the tip length and the tip should be centered at the free end. In this case, to calculate coefficient of friction, friction force should be divided by the sum of applied load and intrinsic adhesive force (Bhushan, 2005). A higher TMR value corresponds to a larger friction force. Friction forces (in Volts) can be converted to force units (in Newtons) and absolute friction forces can be obtained using heavy calibration methods (Bistac & Galliano, 2005). Series of nano-friction measurements were made using pyramidal shaped tips. The Si_3N_4 probe has the same properties of probes used in nano-adhesion, and the same normal spring constant (0.3 N m^{-1}). TMR values have been measured for different applied loads (Volts). The friction properties of different HPMC films were compared using TMR values.

2.6. Adhesion at macroscale: tack test

Adhesion behavior of HPMC films was evaluated with a classical probe tack test (Lakrout, Creton, Ahn, & Shull, 2001). The experiment was performed by putting the HPMC films in contact with a glass substrate, cleaned with ethanol and dried before use. The surface contact area is 3.14 cm^2. The two surfaces were put in contact under a normal force of 10 N. After 5 min of contact time, the two surfaces were separated at a constant velocity of 1 mm s^{-1}. Separation force and energy were measured.

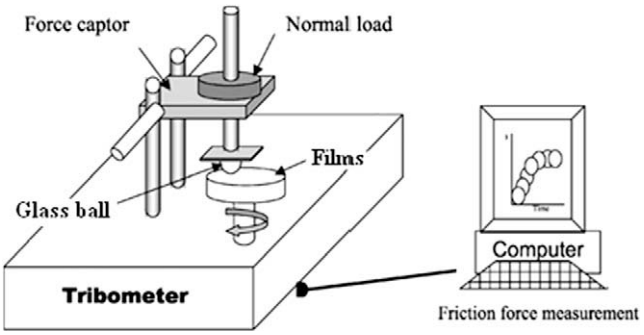

Fig. 3. Pin-on-disk tribometer.

2.7. Friction at macroscale: pin-on-disk tribometer

Tribological investigations of HPMC films at macroscale were carried out on a conventional pin-on-disk tribometer (Fig. 3) by sliding a glass ball (φ = 6 mm) on substrates. The HPMC films were deposited on glass plate, and a glass ball was brought into contact with HPMC films, under a given normal load. The glass plate was then rotated at a given speed and the force opposed to the motion of the ball (tangential force), which corresponds to the friction force, was recorded. The friction coefficient is calculated also automatically by dividing the measured friction force by the specified applied load. The experiment was performed along a distance of 100 mm at a sliding velocity of 5 mm s^{-1} and an acquisition rate of 100 Hz, under a normal load of 2 N, 5 N and 10 N at 25 °C.

3. Results and discussion

3.1. Topography of pure HPMC film and HPMC–stearic acid films

Before studying the adhesive and friction properties at nanoscale, we first explore the surface topography of pure HPMC films. The surface topography was carried out by tapping mode atomic force microscopy (TM-AFM). Fig. 4 represents two AFM images at two different scales of pure HPMC films, 10 μm × 10 μm and 1 μm × 1 μm, respectively.

Phase contrast images represent the phase lag between the piezo excitation oscillation and the tip oscillation. Therefore, such images reveal differences in terms of mechanical and damping properties of the surface. The phase contrast images at large scale (10 μm × 10 μm) reveal the homogeneity of mechanical/chemical properties of the surface. At smaller scale (1 μm × 1 μm), phase lag is very low (<10°), indicating even locally the homogeneity of the film surface. On the other hand, the corresponding topographic image (1 μm × 1 μm) shows the presence of nano-domains, of spherical form, usually called clusters in the literature with a characteristic size 20–30 nm. HPMC nano-domains are due to the existence of aggregates or clusters of HPMC chains in the film-forming solution. The hydrophobic interactions between the hydrophobic substituents of HPMC polymer induce the formation of these clusters (Camino, Pérez, & Pilosof, 2009; Wollenweber, Makievski, Miller, & Daniels, 2000).

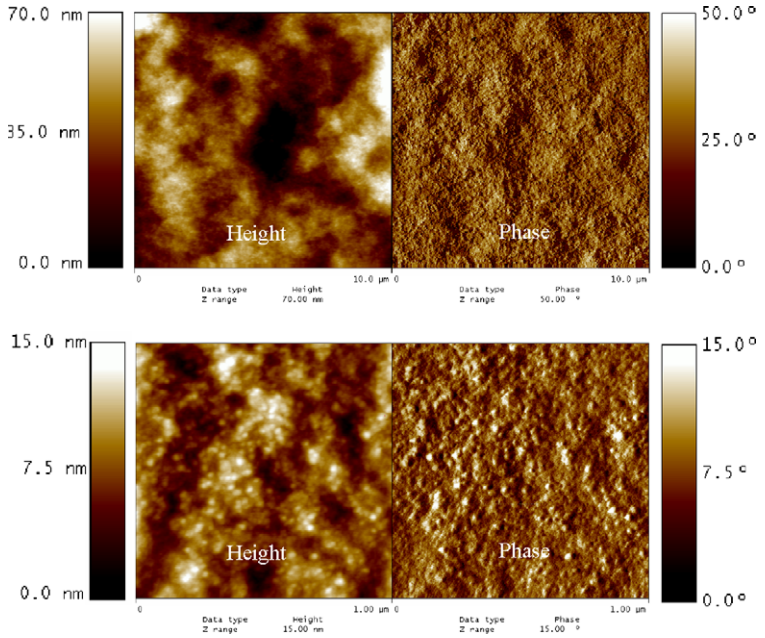

Fig. 4. AFM topographic and phase contrast images at two scales (10 μm × 10 μm) and (1 μm × 1 μm) of pure HPMC film.

Tapping mode AFM analysis of four HPMC film samples with different stearic acid contents indicates a variation of surface topography (Fig. 5). Whereas no contrast was observed on the phase images.

The topographic images and the section analysis show variation of surface aspect. The scan size of each image is 1 μm × 1 μm and the Z-range is 15 nm. Fig. 5a concerns pure HPMC film. Fig. 5b–d are observed for formulated films having stearic acid content equal to 0.1%, 0.5% and 1%, respectively. Average surface roughness, Ra, expressed in nm is also given. R_a values decrease with stearic acid content from 2.3 nm for pure HPMC films to 0.8 nm for films having 1% stearic acid. The granular structure, characteristic of pure HPMC, disappears progressively when stearic acid content increases. This effect is proposed to be due to migration of stearic acid molecules at the film surface (Sebti et al., 2002; Yang & Paulson, 2000). For high stearic acid content, the formation of homogeneous layer is suspected. In this case, the migration of stearic acid (SA) at the surface is possible and results from a phase separation between the hydrophobic additive and the HPMC polymer matrix. To confirm this hypothesis, contact angle measurements and surface free energy determination are necessary to characterize the thermodynamic properties of the film surface.

3.2. Surface properties

The initial surface free energy of pure HPMC films is 43 mJ m^{-2} as determined by wettability measurements. However, this energy is splitted into two components: dispersive (33 mJ m^{-2}) and polar (10 mJ m^{-2}) which respectively represents hydrophobic and

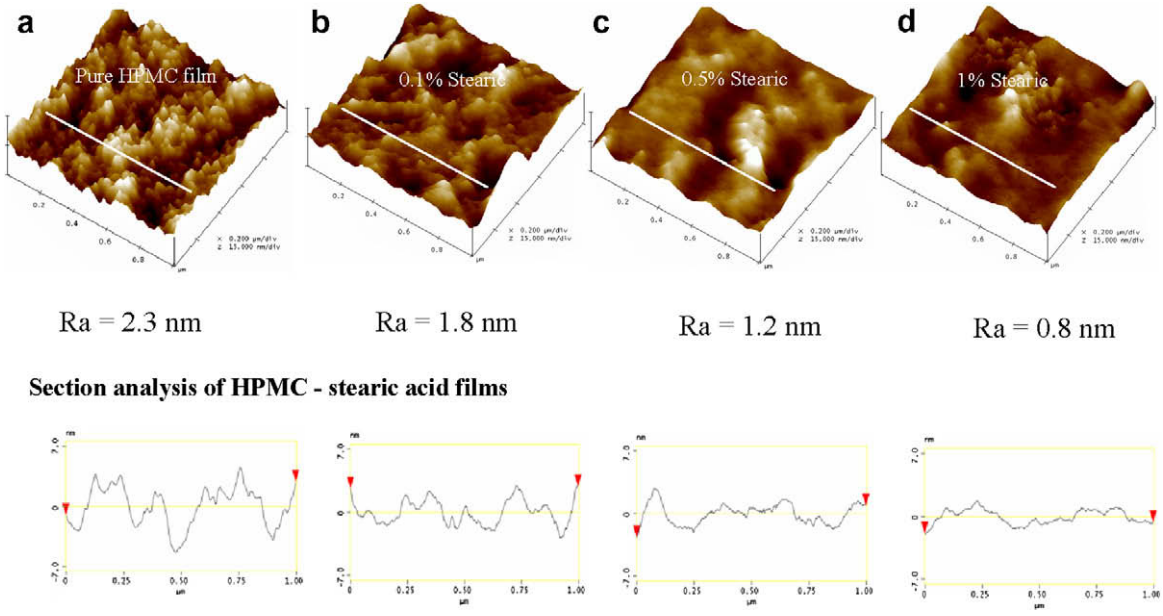

Fig. 5. TM-AFM topographic images (1 μm × 1 μm) and section analysis of HPMC–stearic acid (SA) films. (a) Pure HPMC film, (b) HPMC + 0.1%SA, (c) HPMC + 0.5%SA, (d) HPMC + 1%SA.

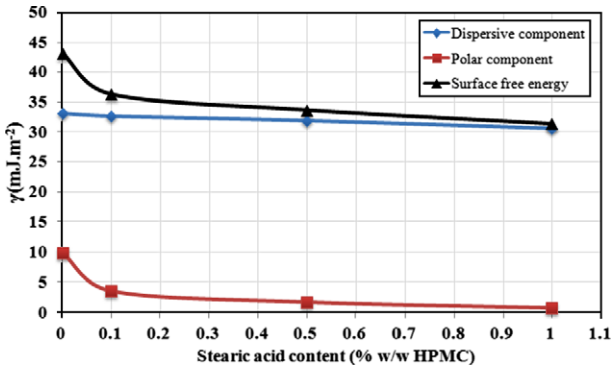

Fig. 6. Surface free energy (mJ m^{-2}), polar and dispersive components versus stearic acid content into HPMC films.

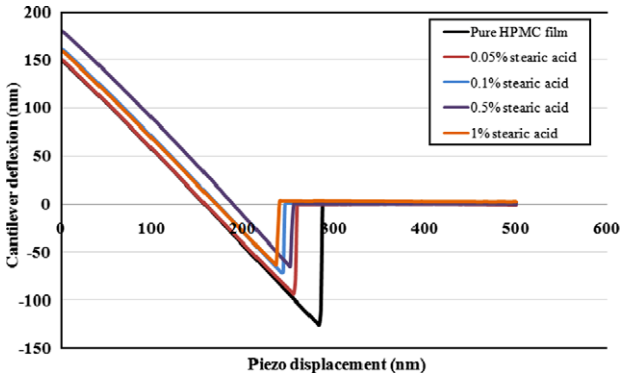

Fig. 7. Force curves (retraction) of different HPMC–stearic acid films.

hydrophilic character of the film surface. Fig. 6 shows the results of surface free energy obtained for formulated films as a function of stearic acid content.

The contribution of polar component γ^p to the total surface free energy of HPMC pure film is equal to 10 mJ m^{-2} which is considerably higher than for HPMC formulated films. This contribution is due to hydrophilic substituents of cellulosic chains (hydroxyl groups) (Luner & Oh, 2001). Even for low stearic acid content (0.1% w/w HPMC), a strong decrease of surface free energy is observed. The water contact angle increases from 69° to 94° with the introduction of 1% (w/w HPMC) stearic acid. As a result, the addition of 1% (w/w HPMC) of stearic acid (γ = 21.8 mJ m^{-2}) decreases the surface free energy to 31.3 mJ m^{-2}. The addition of stearic acid affects significantly the polar component, reflecting therefore the reduction of films hydrophilicity and shows the presence of non-polar aliphatic chains at the film top surface. This first result confirms the hypothesis of stearic acid chain migration and phase separation at the formulated film surface. The difference between the values of surface energy of pure stearic acid and HPMC–stearic acid films is probably due to differences in terms of conformation and surface molecular orientation. Indeed for pure stearic acid thin films, SAMs have been observed (Fowkes, 1969) which is not the case in HPMC formulated films.

3.3. Adhesion at nanoscale

To evaluate nano-adhesion, force–distance curves have been obtained. The maximum cantilever deflection Δz during tip-substrate separation is directly proportional to the adhesion force. Fig. 7 shows the experimental force curves obtained on differents HPMC and HPMC formulated films surfaces having an increasing content of stearic acid.

It is first observed that before tip pull-off the slope of the deflecion–displacement curve is equal to unity for all samples, indicating that no plastic or viscoelastic deformation occurs during tip-film surface contact. Then, during the separation step, a decrease of the pull-off deflecion with hydrophobic character of HPMC film surface is observed. Knowing the spring constant of the cantilever, the adhesion force has been determined by application of Hook's law ($F_{adh} = K \times \Delta z_{(pull\text{-}off)}$) as a function of stearic acid content (Fig. 8). The most important factors which can influence the adhesion forces are the tip-surface interactions and the tip-surface contact area. Since the measurements were made with the same AFM tip (i.e. same radius of curvature at the apex), and the same tip indentation before retraction, only the intensities of the tip-film surface interactions differ between different samples.

Fig. 8 clearly shows that adhesion force at the nanoscale decreases when stearic acid content increases. This result supports, in a quantitative way, the hypothesis of a surface enrichment in hydrophobic species when stearic acid content increases in the HPMC formulated films.

The origin of the measured adhesive force between AFM tip and HPMC films surface are van der Waals force and capillary force. This later is due to water meniscus formation (Israelachvili, 1991, 1995; Liu, Wu, & Evans, 1994). The water present on film surfaces is due to the condensation of water vapor from environment. Then, the total adhesion force is given by the following expression:

$$F_{adh} = F_{VDW} + F_{cap} \quad (3)$$

where F_{VDW} and F_{cap} represent the respective contribution of VDW and capillary forces. The contribution of both forces depends on many factors such as distance between AFM tip-sample surface, surface roughness, hydrophobicity and the relative humidity (Stifter, Marti, & Bhushan, 2000). In our case, the last factor is constant, but the surface roughness and the surface hydrophobic character of HPMC films depend on stearic acid content. As experiences were conducted with the same probe, variation of tip radius is avoided. Furthermore, the dispersive component of surface free energy which is representative of VDW contribution was almost constant with introduction of stearic acid (cf. Fig. 6). However, the attractive capillary force (Riedo, Levy, & Brune, 2002) F_{cap} is given by:

$$F_{cap} = 2\pi R\gamma_1(\cos\theta_1 + \cos\theta_2) \quad (4)$$

where γ_1 is the surface free energy of water in air, θ_1 and θ_2 are the contact angles between the water and the two surfaces (AFM tip and HPMC films). The presence of stearic acid on HPMC films surface generates a hydrophobic surface and as a consequence a reduction of the condensation of water (Laplace pressure) inside AFM tip-HPMC films contact area. This effect induces a decrease of the capillary force F_{cap}, resulting thereafter a decrease of the adhesion force F_{adh} between AFM tip and HPMC films.

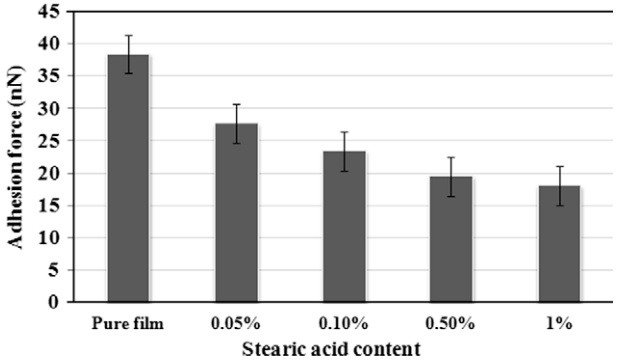

Fig. 8. Adhesion force (nN) versus stearic acid content into HPMC films.

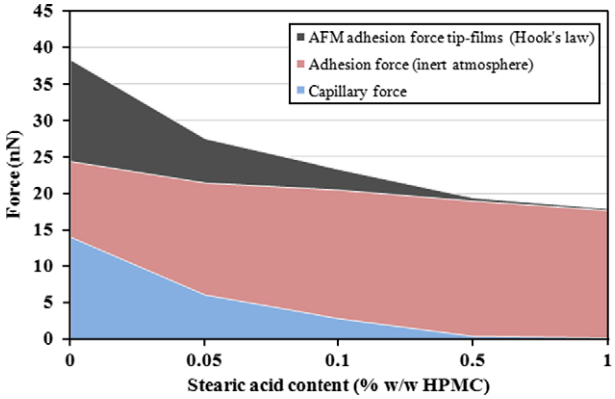

Fig. 9. Contribution of the different surface forces versus stearic acid content in HPMC formulated films.

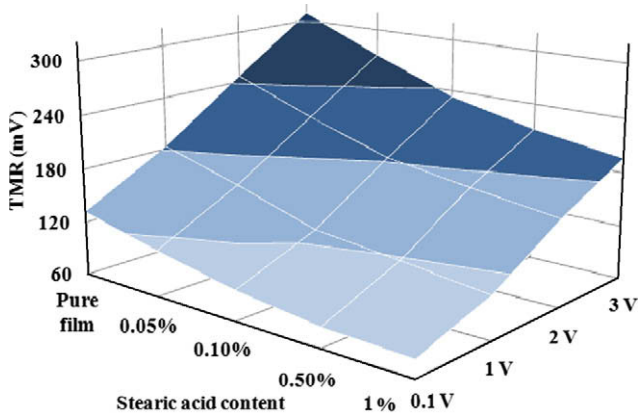

Fig. 10. Variation of TMR versus stearic acid content (% w/w HPMC) and normal load (Volt).

To a first approximation, since HPMC formulated films have a T_g equal to 138 °C and stearic acid has a melting point of 70 °C, one can consider that film surfaces are not deformable and purely elastic at room temperature. Thus, the adhesion force between a non-deformable spherical particle (AFM tip) of radius R and a flat surface (HPMC and HPMC formulated films) in an inert atmosphere is (Israelachvili, 1991):

$$F_{VDW} = 4\pi R\gamma_{SV} \quad (5)$$

In atmosphere containing water vapor, the capillary force must contribute to the expression of the adhesion force according to Eq. (4). Fig. 9 represents, versus stearic acid content (% w/w HPMC), the contribution of both forces (VDW and capillary forces) to the nano-adhesion force between AFM tip-HPMC films. The values of capillary force were deduced by subtracting the adhesion force in inert atmosphere (Eq. (5)) to the adhesion force calculated on the basis of AFM force-curve experiments.

Fig. 9 shows clearly that the decrease of the capillary force is mainly responsible for the decrease of the adhesion force at nanoscale and follows almost the same evolution with addition of stearic acid. The strong decrease of capillary force with 0.1% of stearic acid is remarkable. These results seem in agreement with the tendency observed for the surface free energy decrease and more particularly its polar component, which reflects the absence of dipoles having important polarity. The surface free energy, affected by the presence of hydrophobic stearic acid molecules, has an immediate effect on the adhesion at nanoscale between AFM tip and the surface of HPMC formulated films.

3.4. Adhesion at macroscale: tack test

The tack experiments were performed in ambient air, at room temperature (25 °C). The experiments have shown that HPMC films are non-sticking. The adhesion force at macroscale is indeed about micro-Newtons for pure HPMC film and becomes rather equal to zero for HPMC films containing stearic acid. The extremely low adhesion force generated by the presence of a hydrophobic stearic acid surface layer explains the fact that this macroscale adhesion test is insensitive to force variation in the sub μN domain. Even for very low amount of stearic acid, the adhesion force measured at macroscale is closed to zero. This result supports once more the hypothesis of a hydrophobic layer present at the formulated film surfaces.

General speaking, the results of nano/macro-adhesion present the same tendency with the variation of chemical composition of films. At local scale, the high performance of AFM provides a precise evaluation of any modification of surface properties. At larger scale, since the adhesion force is not important even for pure films (values in μN), the changes induced whatever stearic acid content (in the range 0.05–1%) remain not discriminant.

3.5. Friction at nanoscale

During friction measurements, the friction force data was withdrawn from both the forward (trace T) and backward (retrace R) scans. To study HPMC–stearic acid films nano-friction, the variation of TMR as a function of stearic acid content (% w/w HPMC) at different normal loads (Volt) is summarized in Fig. 10.

It shows that the increase of stearic acid content causes a decrease of the TMR value and thus of the friction force whatever the applied normal load. The higher friction force is measured for pure HPMC films, whatever the applied normal load. This tendency was previously observed for nano-adhesion force which was greater for pure HPMC film surface. Friction seems to be correlated to nano-adhesion. Indeed friction force decreases when stearic acid content increases. One can suspect that the addition of stearic acid into HPMC films increases the contact area between AFM tip and surface, because the surface roughness becomes smoother (cf. Fig. 5). Therefore, the contribution of van der Waals interactions would be greater, but in contrast a strong decrease of capillary forces also occurs when the amount of stearic acid increases. Friction force lowering with stearic acid shows that capillary contribution is the dominant factor. In other words, effect of hydrophobic chains leads to decrease the tip-HPMC films surface interactions and thus leads to low adhesion and friction forces. The migration of stearic acid molecules induces the formation of a lubricant layer at the HPMC film surfaces. These observations indicate that capillary condensation is an important factor in addition to the frictional properties of HPMC formulated films under ambient conditions, which agrees with results obtained for cellulosic films (Garoff & Zauscher, 2002), polymer-coated silicon surface (Ren, Yang, Wang, Liu, & Zhao, 2004) and peptide-containing alkylsiloxane monolayer (Song, Ren, Wang, Yang, & Zhang, 2006).

The increase of applied normal load induces a higher friction force (in agreement with classical Amonton law). The values of TMR versus the applied load are linear for both HPMC and HPMC formulated films. The intercept of the friction force versus normal load line at a 0 V value of applied force corresponds to the adhesion force. TMR values obtained at zero value of normal force are represented in Fig. 11 as a function of stearic acid content. A constant decrease of TMR (at 0 V) is observed.

The evolution of TMR at zero load versus stearic acid content follows the same tendency than previously observed for adhesion

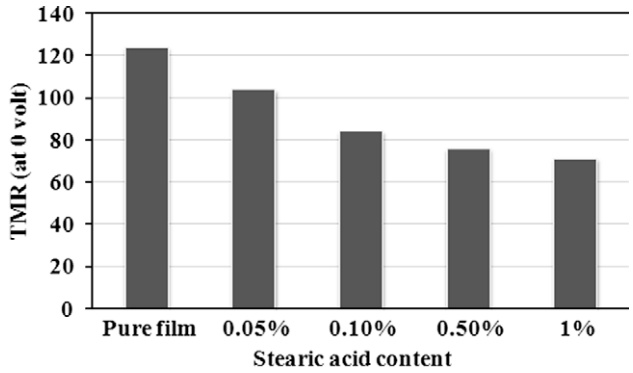

Fig. 11. Variation of TMR (at zero normal load) versus stearic acid content (% w/w HPMC).

force at nanoscale (Fig. 8). As a consequence adhesion and friction mechanisms, at a local scale, must be connected. This fact supports the hypothesis of the formation of a weak boundary layer (WBL) (O'Shea, Welland, & Rayment, 1992) at the film top surface. This later is formed by migration and surface segregation of stearic acid molecules. This weak boundary layer has low cohesion leading to sliding properties during tip-film surface contact and low adhesion (hydrophobic and low molecular weight compared to pure HPMC).

During the measurement of the friction force, the normal load applied to the AFM tip in contact with the film surface plays an important role. The friction force between the film and the tip can affect the surface topography. Fig. 12 shows four surface plots of topographic images (2 μm × 2 μm) obtained by friction force microscopy (FFM) on HPMC films at two different applied normal loads (in Volts).

Although pure HPMC film possesses very low surface deformability, one can see traces of wear generated by AFM tip on pure HPMC surface. Under 3 V normal load, one can observe characteristics scratches patterns (Fig. 12b). On the contrary, for HPMC films formulated with stearic acid, no surface deformation is observed even under high applied load (Fig. 12d) and AFM tip does not damage the films surfaces. Stearic acid is present in the solid state at the interface. Nevertheless, the value of the contact pressure during AFM tip sliding is greater than the cohesive energy of hydrophobic molecules, leading thus to sliding motion of stearic acid molecules. Under this contact pressure, SA plays the role of a lubricant. These films have a better wear resistance and consequently exhibit a lower friction force.

3.6. Friction at macroscale

The macro tribological properties of HPMC films were investigated through the friction of a glass ball on the film surface. The friction coefficients are measured as a function of sliding time and sliding distance. Before each tests, the glass ball was chemically cleaned. Each data is the average value of three measurements. Fig. 13 represents an example of variation of friction coefficient versus the sliding distance (10 cm) for HPMC films having different contents of stearic acid and under an applied load of 2 N, at a sliding velocity of 5 mm s^{-1}.

The average friction coefficient over all the sliding distance is automatically computed on the basis of data like represented in Fig. 13.

In a systematic way, no changes of the friction coefficient with sliding distance are observed at macroscale. Under 2 N applied load, stearic acid has strong effect on the friction coefficient. The friction force decreases dramatically with stearic acid even for very low content (Fig. 13 – 0.05% stearic acid). To study the applied load effect on macro tribological properties of HPMC films, the friction forces were also evaluated at different contents of stearic acid (Fig. 14) under applied loads ranging from 2 to 10 N. The friction forces were calculated using:

$$F_T = \mu \times F_N \quad (6)$$

where F_N is the applied load (N) and μ is the friction coefficient.

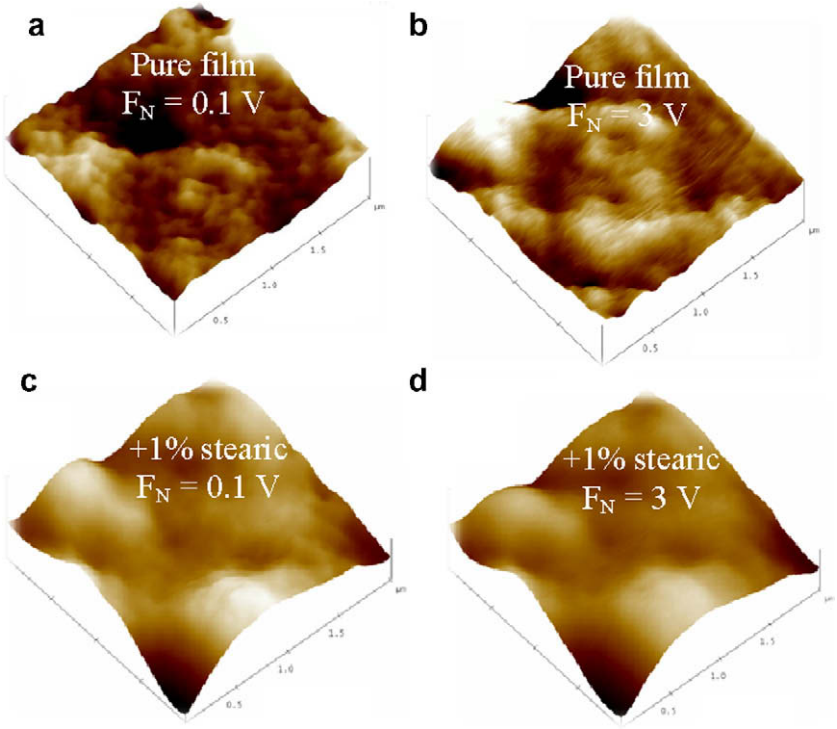

Fig. 12. Topographic images (FFM) (2 μm × 2 μm) of pure HPMC films (a and b), HPMC films with 1% stearic acid SA (c and d).

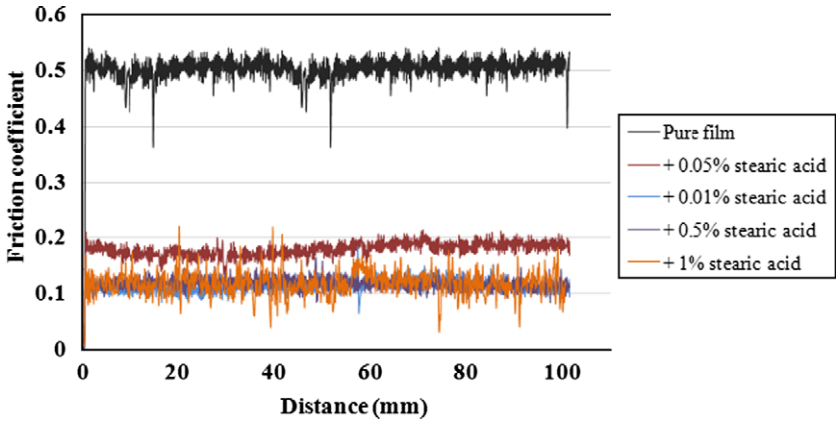

Fig. 13. Friction coefficient versus distance for different HPMC–stearic acid content.

First, one can remark a high dependence of friction force on applied load for pure HPMC films. Moreover, the friction coefficient remains rather constant whatever the applied load in the range 2–10 N. This traduces the high friction coefficient obtained for pure films due to a hydrophilic contact of a polar glass ball with polar HPMC moreover made of long polymer chains having low flexibility, as a consequence adhesion is strong and prevents easy sliding. On the contrary, for HPMC formulated films, the addition of 0.1% (w/w HPMC) of stearic acid is able to almost fix the friction force in the range of applied load used, and very low changes in friction force was observed. For both samples, the mean friction coefficient μ is the slope in the representation of the friction force (N) versus the applied load (N). We found that μ is 0.38 in the case of pure HPMC films. But, with 0.1% of stearic acid (w/w HPMC), the friction coefficient becomes drops to 0.1. The extrapolation of friction force curve at zero normal load shows very low values. Once more these results support the hypothesis of the formation of a weak boundary layer of stearic acid that plays the role of an easy sliding layer. As a consequence the friction coefficient decreases with normal load.

Stearic acid has a great influence on frictional properties at macroscale. Incorporation of stearic acid allows HPMC films to exhibit high sliding characteristic. Its strong effect on HPMC films is believed to be caused by the polar nature of hydroxyl groups on cellulosic chains that induces phase separation and surface migration of stearic acid. In addition, the low molecular weight of the used fatty acid favors surface sliding and thus reduces friction. Finally, these results are in good agreement with adhesion at macroscale performed by tack test and could explain the fact that adhesion of HPMC films containing stearic acid is too low to be quantitatively measured at macroscale.

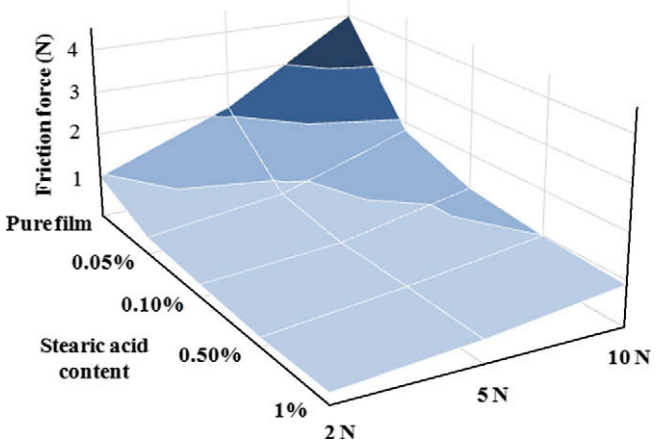

Fig. 14. Variation of friction force versus stearic acid content (% w/w HPMC) and normal load (N).

4. Conclusion

In this study, the adhesion and frictional properties of HPMC formulated films at two different scales were investigated by AFM/FFM, tack test and a ball on disk friction test. Fatty acid, which was incorporated as hydrophobic additive to HPMC films, has a strong effect on surface properties. Logically, lowering of surface free energy by stearic acid incorporation was confirmed by wettability measurements. Using AFM tapping mode, surface topography of HPMC–stearic acid films was analyzed. Cross section plots indicate that average film roughness decreases with stearic acid content. Hypothesis of surface migration of hydrophobic additive is proposed and confirmed by using different experimental studies. Strong coherence between surface free energy and adhesion at nanoscale is observed.

Multi-scale techniques show that surface properties are governed by phase separation between hydrophobic additive and HPMC matrix films, and surface accumulation of stearic acid. The friction force between AFM tip-surface films is highly influenced by surface free energy and adhesion at nanoscale. The experiments revealed that water capillary force has large influence on adhesion and friction at nanoscale.

On the other hand, the macroscopic experimental results show good agreement with those at nanoscale. The macro-friction between a glass ball and the HPMC formulated films surface is also lowered with stearic acid content. Results support the surface migration and surface phase separation phenomenon between polar HPMC matrix and hydrophobic fatty acid. The low molecular weight of stearic acid favors surface sliding and thus reduces friction. The nano/macro properties of HPMC formulated films were strongly dependent on stearic acid content. This study provides evidence of a relationship between adhesion and friction properties into systems where the additive plays an important role as lubricant. On the basis on results obtained, other hydrophobic additives can be used for film coating formulations. Results seem to be transferable, particularly for low or very low amount of hydrophobic additive with a similar film formulation process.

The present study reports pertinent experimental methodology for a characterization of the surface properties of films particularly when they have been formulated for pharmaceutical applications like coatings and free films for encapsulation. In all the cases, the use of multiscales and multitechniques approaches (variety of

probe materials such as water droplet, AFM tip, glass ball, ...) is an essential key to attempt to propose mechanisms of adhesion and friction of complex formulated systems.

Acknowledgement

Authors are grateful to "Région Alsace" for funding of this work.

References

Aulton, M. E., Abdul-Razzak, M. H., & Hogan, J. E. (1981). Thermechanical properties of hydroxypropylmethylcellulose films derived from aqueous systems. *Drug Development and Industrial Pharmacy, 7*, 649–669.

Ayranci, E., & Tunc, S. (2001). The effect of fatty acid content on water vapor and carbon dioxide transmission of cellulose-based edible films. *Food Chemistry, 72*, 231–236.

Bechard, S. R., Quraishi, O., & Kwong, E. (1992). Film coating: Effect of titanium dioxide concentration and film thickness on the photostability of nifedipine. *International Journal of Pharmaceutics, 87*, 133–139.

Bhushan, B. (2005). *Nanotribology and nanomechanics: An introduction*. New York: Springer.

Birdi, K. S. (2003). *Scanning probe microscopes: Applications in science and technology*. Boca Raton, Florida: CRC Press.

Bistac, S., & Galliano, A. (2005). Nano and macro tribology of elastomers. *Tribology Letters, 18*, 21–25.

Brogly, M., Noel, O., Awada, H., Castelein, G., & Schultz, J. (2006). A nanoscale study of the adhesive contact. *Comptes Rendus Chimie, 9*, 99–110.

Camino, N. A., Pérez, O. E., & Pilosof, A. M. R. (2009). Molecular and functional modification of hydroxypropylmethylcellulose by high-intensity ultrasound. *Food Hydrocolloids, 23*, 1089–1095.

Coma, V., Sebti, I., Pardon, P., Deschamps, A., & Pichavant, H. (2001). Anti-microbial edible packaging based on cellulosic ethers, fatty acids and nisin incorporation to inhibit Listeria innocua and Staphylococcus aureus. *Journal of Food Protection, 64*, 470–475.

Debeaufort, F., & Voilley, A. (1997). Methylcellulose-based edible films and coatings: 2. Mechanical and thermal properties as a function of plasticizer content. *Journal of Agricultural and Food Chemistry, 45*, 685–689.

Doelker, E. (1993). Cellulose derivatives. *Advances in Polymer Science, 107*, 199–265.

Ford, J. L. (1999). Thermal analysis of hydroxypropylmethylcellulose and methylcellulose: Powders, gels and matrix tablets. *International Journal of Pharmaceutics, 179*, 209–228.

Fowkes, F. M. (1963). Additivity of intermolecular forces at interfaces. I. Determination of the contribution to surface and interfacial tensions of dispersion forces in various liquids. *Journal of Physical Chemistry, 67*, 2538–2541.

Fowkes, F. M. (1969). In *Hydrophobic surfaces*. New York: Academic Press.

Gad, S. C. (2008). *Pharmaceutical manufacturing handbook: Production and processes*. Hoboken, New Jersey: John Wiley & Sons.

Garoff, N., & Zauscher, S. (2002). The influence of fatty acids and humidity on friction and adhesion of hydrophilic polymer surfaces. *Langmuir, 18*, 6921–6927.

Hagenmaier, R. D., & Shaw, P. E. (1990). Moisture permeability of edible films made with fatty acid and (hydroxy propyl) methylcellulose. *Journal of Agricultural and Food Chemistry, 38*, 1799–1803.

Hutter, J. L., & Bechhoefer, J. (1993). Calibration of atomic-force microscope tips. *Review of Scientific Instruments, 64*, 1868–1873.

Israelachvili, J. N. (1991). *Intermolecular and surface forces* (2nd ed.). London: Academic Press.

Israelachvili, J. N. (1995). Surface forces and microrheology of molecularly thin liquid films. In B. Bhushan (Ed.), *Handbook of micro/nano tribology*. Boca Raton: CRC Press.

Kamel, S., Ali, N., Jahangir, K., Shah, S. M., & El-Gendy, A. A. (2008). Pharmaceutical significance of cellulose: A review. *EXPRESS Polymer Letters, 2*, 758–778.

Lakrout, H., Creton, C., Ahn, D., & Shull, K. R. (2001). Influence of molecular features on the tackiness of acrylic polymer melts. *Macromolecules, 34*, 7448–7458.

Liu, Y., Wu, T., & Evans, D. F. (1994). Lateral force microscopy study on the shear properties of self-assembled monolayers of dialkylammonium surfactant on mica. *Langmuir, 10*, 2241–2245.

Luner, P. E., & Oh, E. (2001). Characterization of the surface free energy of cellulose ether films. *Colloids and Surfaces A: Physicochemical and Engineering Aspects, 181*, 31–48.

McGinity, J. W., & Felton, L. A. (2008). *Aqueous polymeric coatings for pharmaceutical dosage forms* (3rd ed.). New York: Informa Healthcare.

Navarro-Tarazaga, M. Ll., Sothornvit, R., & Pérez-Gago, M. B. (2008). Effect of plasticizer type and amount on hydroxypropyl methylcellulose-beeswax edible film properties and postharvest quality of coated plums (Cv. Angeleno). *Journal of Agricultural and Food Chemistry, 56*, 9502–9509.

Ogura, T., Furuya, Y., & Matsuura, S. (1998). HPMC capsules: An alternative to gelatin. *Pharmaceutical Technology Europe, 10*, 32–42.

Okhamafe, A. O., & York, P. (1983). Analysis of the permeation and mechanical characteristics of some aqueous-based edible films. *Journal of Pharmacy and Pharmacology, 35*, 409–415.

O'Shea, S. J., Welland, M. E., & Rayment, T. (1992). Atomic force microscope study of boundary layer lubrication. *Applied Physics Letters, 61*, 2240–2242.

Ott, E., Spurlin, H. M., & Graffin, M. W. (1954). *High polymers. Cellulose and cellulose derivatives Part 2* (Vol. 5). New York: Interscience.

Owens, D. K., & Wendt, R. C. (1969). Estimation of the surface free energy of polymers. *Journal of Applied Polymer Science, 13*, 1741–1747.

Pérez, O. E., Carrera Sánchez, C., Rodríguez Patino, J. M., & Pilosof, A. M. R. (2006). Thermodynamic and dynamic characteristics of hydroxypropylmethylcellulose adsorbed films at the air–water interface. *Biomacromolecules, 7*, 388–393.

Ren, S. L., Yang, S. R., Wang, J. Q., Liu, W. M., & Zhao, Y. P. (2004). Preparation and tribological studies of stearic acid self-assembled monolayers on polymer-coated silicon surface. *Chemistry of Materials, 16*, 428–434.

Riedo, E., Levy, F., & Brune, H. (2002). Kinetics of capillary condensation in nanoscopic sliding friction. *Physical Review Letters, 88*, 185505–185508.

Sakellariou, P., & Rowe, R. C. (1995). Interactions in cellulose derivate films for oral drug delivery. *Progress in Polymer Science, 20*, 889–942.

Sebti, I., Ham-Pichavant, F., & Coma, V. (2002). Edible bioactive fatty acid-cellulosic derivative composites used in food-packaging applications. *Journal of Agricultural and Food Chemistry, 50*, 4290–4294.

Smith, R. (2005). *Biodegradable polymers for industrial applications*. Cambridge: Woodhead.

Song, S., Ren, S., Wang, J., Yang, S., & Zhang, J. (2006). Preparation and tribological study of a peptide-containing alkylsiloxane monolayer on silicon. *Langmuir, 22*, 6010–6015.

Stifter, T., Marti, O., & Bhushan, B. (2000). Theoretical investigation of the distance dependence of capillary and van der Waals forces in scanning probe microscopy. *Physical Review B, 62*, 13667–13673.

Tahara, K., Yamamoto, K., & Nishihata, T. (1995). Overall mechanism behind matrix sustained release (SR) tablets prepared with hydroxypropyl methylcellulose 2910. *Journal of Controlled Release, 35*, 59–66.

Torii, A., Sasaki, M., Hane, K., & Okuma, S. (1996). A method for determining the spring constant of cantilevers for atomic force microscopy. *Measurement Science and Technology, 7*, 179–184.

Torres, J. A., Motoki, M., & Karel, M. (1985). Microbial stabilization of intermediate moisture food surfaces. I. Control of surface preservative concentration. *Journal of Food Processing and Preservation, 9*, 75–92.

Villalobos, R., Chanona, J., Hernandez, P., Gutiérrez, G., & Chiralt, A. (2005). Gloss and transparency of hydroxypropyl methylcellulose films containing surfactants as affected by their microstructure. *Food Hydrocolloids, 19*, 53–61.

Villalobos, R., Hernandez-Munoz, P., & Chiralt, A. (2006). Effect of surfactants on water sorption and barrier properties of hydroxypropyl methylcellulose films. *Food Hydrocolloids, 20*, 502–509.

Wollenweber, C., Makievski, A. V., Miller, R., & Daniels, R. (2000). Adsorption of hydroxypropyl methylcellulose at the liquid/liquid interface and the effect on emulsion stability. *Colloids and surfaces A: Physicochemical and Engineering Aspects, 172*, 91–101.

Yang, L., & Paulson, A. T. (2000). Effect of lipids on mechanical and moisture barrier properties of edible gellan film. *Food Research International, 33*, 571–578.